

# <sup>18</sup>F-FDG PET SUVmax Correlates with Osteosarcoma Histologic Response to Neoadjuvant Chemotherapy: Preclinical Evaluation in an Orthotopic Rat Model

Aurélie Dutour<sup>1,3</sup>, Anne-Valérie Decouvelaere<sup>\*2,3</sup>, Jacques Monteil<sup>\*4</sup>, Marie-Eve Duclos<sup>5</sup>, Olivier Roualdes<sup>5</sup>, Raphaël Rousseau<sup>\*1,3,5,6</sup>, and Perrine Marec-Bérard<sup>\*3,6</sup>

<sup>1</sup>Inserm, U590, Lyon, France; <sup>2</sup>Département d'Anatomopathologie et Cytologie, Lyon, France; <sup>3</sup>Centre Léon Bérard, Lyon, France; <sup>4</sup>Service de Médecine Nucléaire, Centre Hospitalier Universitaire Dupuytren, Limoges, France; <sup>5</sup>Université de Lyon, Lyon, France; and <sup>6</sup>Institut d'Hématologie-Oncologie Pédiatrique, Lyon, France

Assessment of osteosarcoma response to neoadjuvant chemotherapy is performed by histopathologic analysis after surgical resection of the primary tumor. The purpose of this study was to evaluate whether <sup>18</sup>F-FDG PET could be a noninvasive surrogate to histopathologic analysis and allow for earlier response evaluation to neoadjuvant chemotherapy in osteosarcoma.

**Methods:** Metabolic response to neoadjuvant chemotherapy was assessed in immunocompetent rats with a preestablished orthotopic osteosarcoma using <sup>18</sup>F-FDG PET before and after receiving 2 doses of ifosfamide. Comparison was then made by assessing histologic responses on euthanized animals. **Results:** Maximum standardized uptake value (SUVmax) measured by <sup>18</sup>F-FDG PET after 2 doses of chemotherapy was correlated to histologic classification ( $P < 0.01$ ). An SUVmax less than 15 corresponded to good responders, whereas an SUVmax greater than 15 but less than 20 and an SUVmax greater than 20 corresponded to partial responders or nonresponders, respectively. A 40% decrease in SUVmax between the first and second <sup>18</sup>F-FDG PET scans distinguished between partial and good response to chemotherapy. **Conclusion:** Determination of SUVmax using semiquantitative <sup>18</sup>F-FDG PET predicts response to neoadjuvant chemotherapy earlier than does histologic analysis.

**Key Words:** osteosarcoma; histologic response; <sup>18</sup>F-FDG PET; metabolic response; SUVmax

J Nucl Med 2009; 50:1533-1540

DOI: 10.2967/jnumed.109.062356

Although it accounts for only 0.1% of all tumors in this age group, osteosarcoma is the most frequent primary malignant bone tumor in children and adolescents (1). The introduction of multiple-agent chemotherapy regimens,

combined with wide-margin, limb-sparing surgery, improved the outcome for these patients, and most modern series report relapse-free survival over 5 y in approximately 65% of patients (2). Whereas the tumor size, location, and presence of metastases at diagnosis carry a prognostic value for patient outcome, the most determining prognostic factor in osteosarcoma remains the response to neoadjuvant chemotherapy. A greater degree of tumor necrosis at the completion of neoadjuvant chemotherapy is associated with a significantly higher survival rate (3). Tumor response to chemotherapy is evaluated at the time of surgery on the resected tumor by histologic analysis according to a method described by Huvos et al. (4). Ninety-five percent or higher tumor necrosis is considered good response to therapy (4). Conversely, a necrosis rate between 90% and 95% is classified as partial response, and tumor necrosis less than 90% qualifies as nonresponder to neoadjuvant chemotherapy (4). Early determination of tumor response during the course of neoadjuvant chemotherapy could prove critical to the detection of nonresponders and offer alternative chemotherapy regimens. The application of noninvasive imaging to determine tumor response to chemotherapy throughout the treatment has been investigated. So far, the value of noninvasive CT or MRI to predict histopathologic treatment responses has failed to demonstrate its benefit during neoadjuvant chemotherapy of musculoskeletal sarcoma (5). CT or MRI changes observed in soft tissues and bone revealed inconsistent correlation with patient outcomes. Moreover, limitations appeared with these techniques when trying to distinguish necrotic tumor, local inflammatory reaction, or fibrotic scarring from residual tumor tissue (6,7). Because <sup>18</sup>F-FDG PET distinguishes metabolic highly active from less-active tumor tissues and can discriminate normal from tumor cells on the basis of glucidic alterations, functional response measured by <sup>18</sup>F-FDG PET may represent a surrogate to histologic tumor response to therapy. Ultimately, treatment may be

Received Jan. 20, 2009; revision accepted Jun. 4, 2009.

For correspondence or reprints contact: Raphaël Rousseau, Institut d'Hématologie-Oncologie Pédiatrique, 1 Place Du Professeur Joseph Renaut, 69373 Lyon, Cedex 08, France.

E-mail: dutoura@lyon.fnclcc.fr

\*Contributed equally to this work.

COPYRIGHT © 2009 by the Society of Nuclear Medicine, Inc.

adapted at an earlier stage during the course of neoadjuvant chemotherapy on the basis of tumor functional activity measured by  $^{18}\text{F}$ -FDG PET rather than volumetric analysis using CT or MRI (8). A decrease in standardized uptake values (SUVs) has been shown to predict response to therapy in malignant lymphomas and other solid tumors (8–11). In soft-tissue sarcomas and gastrointestinal stromal tumors (GIST), metabolic imaging with  $^{18}\text{F}$ -FDG PET allows for the assessment of tumor response to therapy (9,10). Moreover, maximum SUV (SUV<sub>max</sub>) measured by  $^{18}\text{F}$ -FDG PET is correlated to histologic tumor response in patients undergoing neoadjuvant chemotherapy for Ewing sarcoma (12,13). Nonetheless, evidence of the predictive value of  $^{18}\text{F}$ -FDG PET is lacking in osteosarcoma.

Because ethical, financial, and technical constraints make the prospective evaluation of the risk–benefit ratio of  $^{18}\text{F}$ -FDG PET in a pediatric patient population cumbersome, we decided to study the technique in an orthotopic osteosarcoma model in rats. We have previously demonstrated in this model the ability of  $^{18}\text{F}$ -FDG PET to correlate metabolic to histologic responses, thus allowing longitudinal *in vivo* assessment of tumor response to therapy (14,15). We now report data supporting that the  $^{18}\text{F}$ -FDG PET response predicts the histopathologic response to neoadjuvant chemotherapy.

## MATERIALS AND METHODS

### Osteosarcoma Model and Treatment Schedule

Care of and procedures for animals were performed according to institutional and national guidelines. Animals were anesthetized throughout all surgical and imaging procedures with isoflurane/oxygen (2.5%/2.5%, v/v) (Minerve). The transplantable orthotopic and metastatic rat osteosarcoma has been described elsewhere (14,16). This model mimics its human counterpart in terms of aggressiveness, metastatic spreading, and chemoresistance phenotype (15,16). Tumors were grafted on 25-d-old Sprague–Dawley rats (Charles River Laboratories) as previously described (14). Fourteen days after tumor transplantation, animals underwent a first  $^{18}\text{F}$ -FDG PET scan and were randomly assigned to a control (saline,  $n = 10$ ) or a treatment (ifosfamide; Baxter) group ( $n = 10$ ). Treated animals received 2 subcutaneous doses (20 mg/kg each) of ifosfamide 7 d apart (at days 15 and 22 after tumor transplantation). A second  $^{18}\text{F}$ -FDG PET scan was obtained 7 d after the second administration of ifosfamide (i.e., day 29 after tumor implantation). Total tumor volume and metabolic volume were measured using a volume of interest (VOI)–based method on reconstructed PET images. All animals were euthanized if they showed any signs of distress. At the time of necropsy, tumors and lungs were collected for histologic examinations.

### Metabolic Response to Chemotherapy Using $^{18}\text{F}$ -FDG Small-Animal PET Scan

The initial  $^{18}\text{F}$ -FDG PET scan was obtained 14 d after tumor implantation (i.e., 24 h before treatment initiation, or prechemotherapy PET). A second  $^{18}\text{F}$ -FDG PET scan was acquired 7 d after the completion of chemotherapy (i.e., 29 d after tumor transplantation, or postchemotherapy PET). After the animals had fasted for 4 h, they received intravenous injections of  $^{18}\text{F}$ -FDG (30 MBq/kg; CERMEP) 2 h before image acquisition. During acquisition, animals were kept under general anesthesia with isoflurane/oxygen (2.5%/2.5%, v/v), and animals' body temperature was maintained using a warming pad. PET scans were obtained at the Animage core facility on a small-animal PET camera (Clearpet; Raytest). Whole-body images were acquired with 2 bed positions (field of view, 110 mm): one centered on the tumor and the other one on the lungs, with an acquisition time of 15 min per bed position.

Data were processed without attenuation correction, and images were reconstructed using an iterative method (maximum-likelihood expectation maximization, 20 iterations) using the Amide software (<http://amide.sourceforge.net>).  $^{18}\text{F}$ -FDG PET images were semiquantitatively analyzed using a VOI-based method. Ellipsoid VOIs were drawn over the whole tumor. Three-dimensional isocontour VOIs using a 40% maximum threshold defined the total tumor volume. Similarly, a 50% maximum threshold defined the metabolic tumor volume. The 40% and 50% threshold values applied to define the total tumor volume and the metabolic tumor volume in 3-dimensional isocontour VOIs were chosen on the basis of published studies (17,18). As internal negative control, a reference nontumor VOI was positioned in a corresponding location to the tumor region of interest (e.g., in the contralateral unaffected paw). An SUV<sub>max</sub> normalized to body weight was calculated for all volumes using the formula (18):

$$\text{SUV} = \frac{\text{ROI decay-corrected activity/tissue}}{\text{Injected } ^{18}\text{F-FDG dose/body weight}}$$

The 50% and 40% threshold values allowed us to calculate a metabolic volume corresponding to all the voxels having an SUV greater than or equal to 50% and 40% threshold values and to give an SUV mean value for the concerned volume. With this method, the necrotic areas (for which SUVs were below the threshold values) did not affect the metabolic volume measure.

According to recommendations by the European Organization for Research and Treatment of Cancer (EORTC) (19), we graded metabolic responses on the basis of the changes of SUV<sub>max</sub> measured on prechemotherapy PET and postchemotherapy PET reconstructed images (Table 1).

### Histology

All animals were euthanized 24 h after the postchemotherapy PET scan. Primary tumor and lungs were fixed in 10% buffered

**TABLE 1.** Metabolic Response Criteria According to Recommendations of EORTC

SUV change	Metabolic response
SUV increase > 25% within tumor region	Progressive metabolic disease
SUV increase < 25% or SUV decrease < 15%	Stable metabolic disease
SUV decrease > 25%	Partial metabolic response
Complete resolution of $^{18}\text{F}$ -FDG uptake within tumor volume	Complete metabolic response

Remaining viable tumor cells	Histologic response
Viable cells < 5%	Good responder, grade 1
5% < viable cells < 10%	Partial responder, grade 2
Viable cells > 10%	Nonresponder, grade 3
Viable cells > 40%	Nonresponder, grade 4

formalin and then processed and embedded in paraffin. Viable tumor remaining after chemotherapy was expressed as the percentage of whole tumor volume using the Huvos histologic response (Table 2) (4,20). Tumors were oriented, and series of whole transverse sections were cut in the distal fourth, middle, and proximal fourth of the tumor. After hematoxylin and eosin coloration, tissue slides were analyzed using a DM4500 B microscope (Leica). We examined all cases to evaluate the following histologic features: mitotic rate expressed as the number of mitotic figures per 10 high-power fields (1 field, 0.237 mm<sup>2</sup>), necrosis, and bone. For each tumor, mitotic rate and necrosis were estimated on whole transverse sections from the 3 areas (e.g., distal fourth, middle, and proximal fourth of the tumor).

### Immunohistochemistry

Glucose transporter 1 (Glut-1) immunostaining was performed on deparaffinized tumor sections with an anti-rat Glut-1 rabbit polyclonal antibody (Abcam; 1-h incubation at room temperature). Slides were then washed twice in 0.3% phosphate-buffered saline containing bovine serum albumin for 5 min. Slides were incubated with a biotinylated secondary antibody (Vector Laboratories) according to the manufacturer's instructions. After a final wash, tumor sections were stained with a Vectastain ABC Kit (Vector Laboratories), followed by counterstaining using hematoxylin (Sigma-Aldrich) and microscopic examination. Glut-1 staining was graded as positive or negative. Cases were considered negative when less than 10% of cells showed Glut-1 staining and positive when 10% or more of tumor cells showed Glut-1 staining. Variations in staining intensity of the cells were scored, and the following criteria were used: +, weak but unequivocal staining in

some cells; ++, staining of moderate intensity; and +++, strong or intense staining.

### Statistical Analysis

SUVs and tumor volumes were compared between control and treatment groups using a 2-tailed Student *t* test.

Relative mean tumor volume (RMTV) and tumor volume inhibition rate (IR) were calculated as indicated below:

$$\text{RMTV} = (\text{postchemotherapy mean tumor volume} / \text{prechemotherapy mean tumor volume}), \text{ and}$$

$$\text{IR} = \left[ \frac{(\text{RMTV})_{\text{ifosfamide-treated group}}}{(\text{RMTV})_{\text{control group}}} \right] \times 100.$$

*P* values less than 0.01 were considered statistically significant. Correlation between tumor responses determined by histologic analysis or by <sup>18</sup>F-FDG PET was assessed using the Pearson test. Statistical analysis was performed using the StatView 5.0 software package (SAS Institute Inc.).

## RESULTS

### Ifosfamide Induces Clinical and Histologic Tumor Response in Orthotopic Osteosarcoma in Rats

There was no difference in the mean ( $\pm$ SD) tumor volumes measured on <sup>18</sup>F-FDG PET reconstructed images at the initiation of treatment between control and treated animals (1,909  $\pm$  515 mm<sup>3</sup> and 2,559  $\pm$  1,046 mm<sup>3</sup>, respectively; *P* = 0.09). After the end of treatment, the mean tumor volume in the treated animals was significantly smaller than that in the control group (1,251  $\pm$  701 mm<sup>3</sup> vs. 9,172.1  $\pm$  2,693 mm<sup>3</sup>; *P* < 0.01). Compared with the control group, in the treatment group the 2 cycles of ifosfamide induced a 53.34% decrease in tumor volume, which corresponded to a 10.2-fold inhibition rate (*P* < 0.01) (Table 3). According to Huvos histologic response, animals from the control group were all classified as grade 3 or 4 nonresponders (Table 4). In treated animals, histologic evaluation found only good (grade 1, *n* = 5) and partial responders (grade 2, *n* = 5) (Table 4).

Parameter	Control group ( <i>n</i> = 10; mean $\pm$ SD)	Ifosfamide-treated group ( <i>n</i> = 10; mean $\pm$ SD)
Prechemotherapy <sup>18</sup> F-FDG PET		
Total tumor volume (mm <sup>3</sup> )	1,909 $\pm$ 515	2,559 $\pm$ 1,046
Metabolic tumor volume (mm <sup>3</sup> )	1,658 $\pm$ 259, 86.9% of whole tumor	2,418 $\pm$ 288, 94.5% of whole tumor
SUVmax	22 $\pm$ 2.5	28.1 $\pm$ 4.1
Mean SUV	13.6 $\pm$ 1.2	14.2 $\pm$ 1.4
Postchemotherapy <sup>18</sup> F-FDG PET		
Total tumor volume (mm <sup>3</sup> )	9,172 $\pm$ 2,693	1,251 $\pm$ 701
Metabolic tumor volume (mm <sup>3</sup> )	5,650 $\pm$ 1,973, 61.6% of whole tumor	740 $\pm$ 291, 59.2% of whole tumor
SUVmax	25.4 $\pm$ 4.4	16.1 $\pm$ 4.7
Mean SUV	11.9 $\pm$ 1.8	7.5 $\pm$ 1.2
Chemotherapy-induced changes		
Relative mean tumor volume	+401% $\pm$ 157%	-53.34% $\pm$ 13.5%
Tumor volume inhibition rate	—	10.17

**TABLE 4.** Changes in Tumor Volume and SUVs on <sup>18</sup>F-FDG PET Before and After Chemotherapy: Status of Metabolic Response (According to EORTC) and Histologic Response in Control and Ifosfamide-Treated Rats

Group	Rat ID	Prechemotherapy SUVmax	Postchemotherapy SUVmax	Relative SUVmax change	Prechemotherapy total tumor volume (mm <sup>3</sup> )	Postchemotherapy total tumor volume (mm <sup>3</sup> )	Relative tumor volume change	Metabolic response	Histologic response
Control	A-2	21.4	21.3	0%	2,886	8,093	180%	SMD	3 (10%–40%)
	A-3	21.1	23.7	12%	2,200	10,280	367%	SMD	3 (10%–40%)
	A-5	21.1	33.1	57%	2,006	5,517	175%	PMD	3 (10%–40%)
	A-6	23.6	22.6	-4%	1,122	5,134	358%	SMD	3 (10%–40%)
	A-7	23.3	20.7	-11%	1,659	8,506	413%	SMD	3 (10%–40%)
	A-1	20.3	30.7	51%	2,309	9,203	299%	PMD	4 (>40%)
	A-4	20.8	23.1	11%	1,918	12,909	573%	SMD	4 (>40%)
	A-8	14.8	23.0	55%	1,953	13,367	584%	PMD	4 (>40%)
	A-9	20.8	27.7	31%	1,828	10,129	454%	PMD	4 (>40%)
	A-10	19.0	30.6	61%	1,210	8,590	610%	PMD	4 (>40%)
	Mean values	20.6 (±2.4)	25.7 (±4.5)	26% (±28)	1,909.1 (±515)	9,172 (±2,692)	401% (±157)		
Ifosfamide	B-1	25.2	11.8	-53%	2,635	1,680	-36%	PMR	1 (<5%)
	B-2	30.1	12.9	-57%	1,923	1,265	-34%	PMR	1 (<5%)
	B-4	27.3	10.4	-62%	1,844	733	-60%	PMR	1 (<5%)
	B-5	24.7	13.2	-47%	3,025	1,365	-55%	PMR	1 (<5%)
	B-6	32.2	13.1	-59%	1,435	492	-66%	PMR	1 (<5%)
	B-3	21.6	15.6	-28%	926	264	-71%	PMR	2 (5%–10%)
	B-7	33.0	20.3	-38%	4,427	2,719	-39%	PMR	2 (5%–10%)
	B-8	28.7	20.5	-29%	3,247	1,727	-47%	PMR	2 (5%–10%)
	B-9	34.5	26.3	-24%	3,461	1,184	-66%	PMR	2 (5%–10%)
	B-10	23.7	17.1	-28%	2,669	1,082	-59%	PMR	2 (5%–10%)
	Mean	28.1 (±4.3)	16.1 (±5)	-43% (±15)	2,559 (±1,046)	1,251 (±701)	-53% (±3)		

Metabolic response as evaluated according to EORTC: PMD = progressive metabolic disease (tumor SUV increase > 25%); SMD = stable metabolic disease (tumor SUV increase < 25% or tumor SUV decrease < 15%); PMR = partial metabolic response (tumor SUV decrease > 25%). Relative SUVmax change was calculated for each animal as follows: [(postchemotherapy SUVmax - prechemotherapy SUVmax)/prechemotherapy SUVmax] × 100.

### **<sup>18</sup>F-FDG PET Correlates with Histologic Observations in Osteosarcoma in Rats**

For all animals, the SUVmax was observed within the tumor metabolic volumes. Before treatment initiation, the metabolic volume represented 86.9% ( $\pm 13\%$ ) and 94.5% ( $\pm 11\%$ ) of the whole tumor volume in the control and treatment groups, respectively (Table 3). After treatment, the metabolic volume still represented approximately 60% of tumor volume in both groups (Table 3). For all control animals (representative images shown in Fig. 1), when <sup>18</sup>F-FDG PET images were superimposed onto the corresponding whole-mount tumor sections, areas of metabolic volume defined on <sup>18</sup>F-FDG PET images were found to match with the histologically defined hyperproliferative regions (Figs. 1A and 1B). On histologic analysis, these areas presented with the highest cell density, an elevated mitotic score, and a strong staining of Glut-1 (Figs. 1C and 1E). Conversely the areas with the lowest SUV corresponded to tumor regions with necrotic or osteoid areas with low cellular density and weak Glut-1 staining (Figs. 1D and 1F).

Among the treated animals, <sup>18</sup>F-FDG PET scans obtained after the completion of treatment revealed tumors with areas of intense <sup>18</sup>F-FDG fixation (Figs. 2A and 2B) amid areas of lower intensity (Figs. 2A and 2E). The superimposition of <sup>18</sup>F-FDG PET transverse sections with the corresponding whole-mount paraffin slides revealed that the areas showing the least <sup>18</sup>F-FDG fixation intensity (i.e., areas with SUV < SUV mean) corresponded on histologic analysis to necrotic areas. Interestingly, areas of active metabolic activity as visualized by <sup>18</sup>F-FDG PET corresponded on histologic slides to tumor foci as small as 1.2 mm in diameter (Fig. 2C). These remaining tumor foci presented with the same characteristics as the metabolic volume areas of tumors from the control group: high cell density, high mitotic index, and intense expression of Glut-1, all being evidence of the aggressiveness of remaining tumor cells (Figs. 2C and 2D). Areas presenting with an intermediate fixation of <sup>18</sup>F-FDG (areas with SUVs approaching the SUV mean) on <sup>18</sup>F-FDG PET were found to correspond histologically to regions of chemotherapy-induced modifications (Figs. 2E and 2F). No viable tumor cells were found in these areas, but fibrous scarring and infiltration by immune and giant cells were observed (Fig. 2F). These cells presented a Glut-1 staining of moderate intensity. Indeed, normal immune cells are known to express Glut-1, albeit at a lower level than tumor cells, which may explain this nonspecific <sup>18</sup>F-FDG uptake (Fig. 2G).

### **Evaluation of Tumor Response by <sup>18</sup>F-FDG PET**

There was no correlation between changes in tumor volumes (whole or metabolic; Table 4) and histologic responses (Fig. 3), even if a 55% reduction in tumor volume could identify good responders. When applying the criteria of the EORTC to evaluate the tumor metabolic response in our tumor model, all tumors in the control

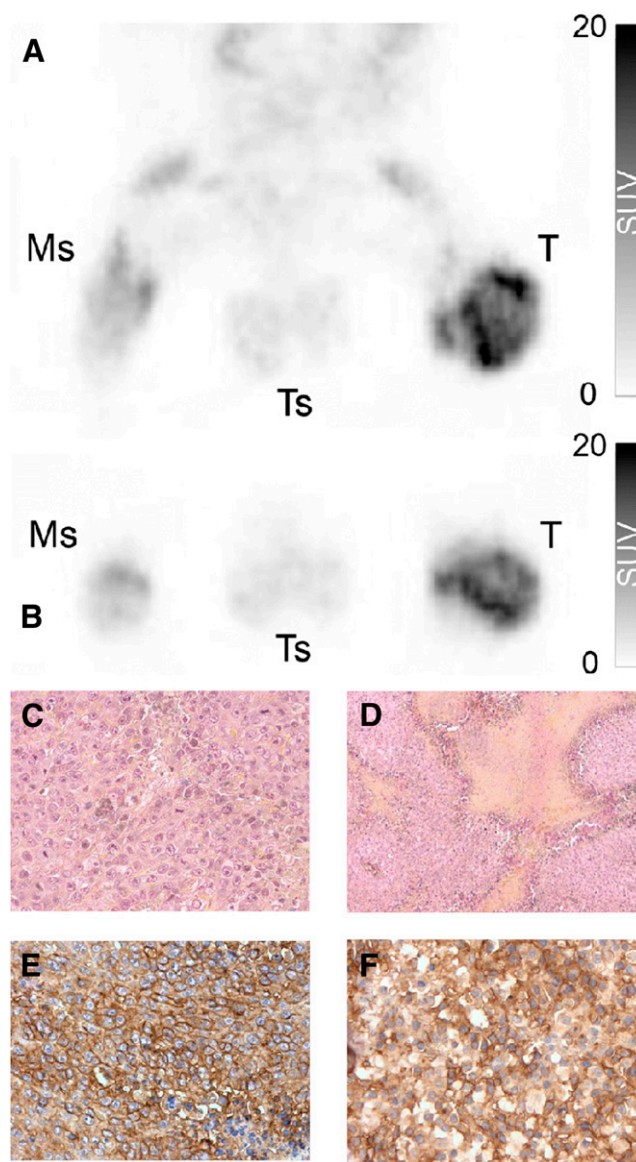
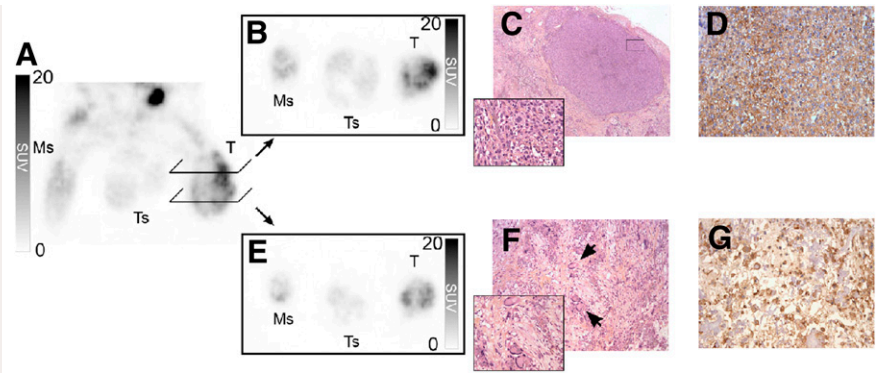


**FIGURE 1.** Representative 3-dimensional maximal-intensity-projection reconstruction obtained for control group. Tumor coronal (A) and transaxial (B) slices visualized by <sup>18</sup>F-FDG PET. Areas with higher fixation of <sup>18</sup>F-FDG corresponded on hematoxylin- and eosin-stained tumor transverse sections (C) to regions with high cellular density, mitotic score, and high homogeneous expression of Glut-1 visualized by immunohistostaining (E). Areas with lower fixation of <sup>18</sup>F-FDG corresponded on hematoxylin- and eosin-stained tumor transverse sections (D) to necrotic areas, or regions with low cellular density, mitotic score, and lower and heterogeneous expression of Glut-1 visualized by immunohistostaining (F). Ms = muscle; T = tumor; Ts = testis. All images are obtained from same rat. Magnifications are  $\times 200$  for C, D, and F;  $\times 100$  for E.

group qualified as progressive disease, whereas all animals in the treated group were considered partial responders (Table 4). No correlation was found between the metabolic response graded according to the recommendations by the EORTC and the histopathologic gradation. Thus, using the

**FIGURE 2.** Representative 3-dimensional maximal-intensity-projection coronal reconstruction of  $^{18}\text{F}$ -FDG PET images from ifosfamide-treated group (A).  $^{18}\text{F}$ -FDG accumulates heterogeneously in tumor. Transaxial slice from region of 1.2-mm thickness showing high levels (B) of  $^{18}\text{F}$ -FDG uptake corresponded on hematoxylin and eosin histologic analysis to remaining hyperproliferative osteosarcoma (C) with strong Glut-1 immunostaining (D). Transaxial slice from region showing low and heterogeneous fixation of  $^{18}\text{F}$ -FDG (E) corresponded on hematoxylin and eosin histologic analysis to chemotherapy-modified regions without viable tumor cells but with infiltration of giant polynuclear immune cells (arrows) (F) expressing Glut-1 (G). Ms = muscle; T = tumor; Ts = testis. Magnifications:  $\times 50$  for C;  $\times 100$  for D and F;  $\times 400$  for G and insets from C and F.



criteria of the EORTC for SUV changes and staging of metabolic response, we could not discriminate good from partial responders (Table 4). A closer analysis of the SUVmax revealed that a 40% decrease in the SUVmax between prechemotherapy and postchemotherapy  $^{18}\text{F}$ -FDG PET could differentiate good from partial responders with a 100% sensitivity and specificity (Fig. 4A). We also found that an SUVmax less than 15 on  $^{18}\text{F}$ -FDG PET performed after chemotherapy distinguished good from partial responders (Fig. 4A). Indeed, 5 of the 5 good responders had a postchemotherapy SUVmax less than 15, whereas animals presenting a partial response to ifosfamide had an SUVmax between 15 and 20 ( $P < 0.01$ ). The SUVmax in rats with progressive tumors (control group,  $n = 10$ ) was above 20; the most aggressive tumor presented with an SUVmax greater than 25 ( $P < 0.01$ ). Interestingly, there was a significant correlation between the SUVmax on

$^{18}\text{F}$ -FDG PET after chemotherapy and histologic response ( $P < 0.01$ ,  $R^2 = 0.94$ ) (Fig. 4B).

## DISCUSSION

In osteosarcoma, response to neoadjuvant chemotherapy is considered complete if less than 5% of viable tumor cells are present on histologic analysis of the resected tumor. Correlation between histologic response to treatment and survival is now widely accepted in patients with bone sarcomas (3,21). Nonetheless, assessing tumor response (or lack thereof) early into neoadjuvant chemotherapy is critical to adapting treatment strategies.

In this study, we evaluated the potential of  $^{18}\text{F}$ -FDG PET as an early predictor of osteosarcoma response to chemotherapy in osteosarcoma-bearing rats treated with 2 doses of ifosfamide. We showed a significant correlation between the SUVmax measured by  $^{18}\text{F}$ -FDG PET after completion of chemotherapy and histologic response evaluated according to Huvos. We established that a cutoff value of 40% between pre- and posttreatment SUVmax discriminated between good and partial responders.

Metabolic imaging using  $^{18}\text{F}$ -FDG PET scans has an established role in staging, predicting the aggressiveness, and detecting the recurrence of many tumors including bone sarcomas (22,23). One of the advantages of  $^{18}\text{F}$ -FDG PET is that it can visualize and quantify  $^{18}\text{F}$ -FDG uptake to distinguish metabolically highly active from less active tumor tissues.  $^{18}\text{F}$ -FDG PET could be useful for the early assessment of tumor response to chemotherapy and the detection of metabolic alterations of tumor cells occurring before alterations in tumor size. Studies conducted in patients with lung, breast, or ovarian cancer and lymphoma have demonstrated that reduced  $^{18}\text{F}$ -FDG uptake can identify responders early after treatment and that increased  $^{18}\text{F}$ -FDG uptake after treatment was associated with a high risk for early disease recurrence and poor prognosis (24,25). The role of  $^{18}\text{F}$ -FDG PET in monitoring response to chemotherapy has been shown in patients with soft-tissue

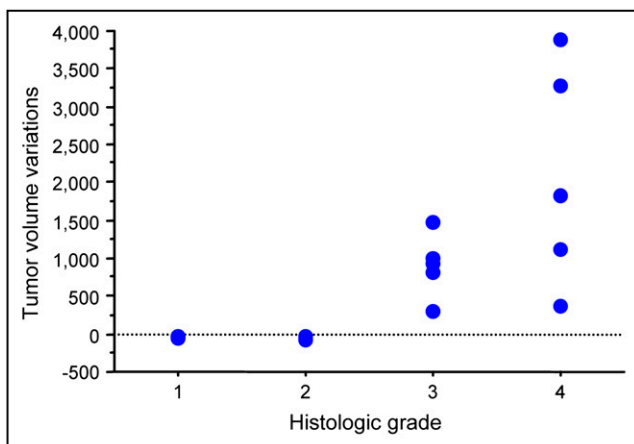


**FIGURE 3.** Scatter plot of histologic response and total tumor volume changes measured using  $^{18}\text{F}$ -FDG PET shows absence of correlation between parameters measured by metabolic imaging and histologic response ( $R^2 = 0.56$ ). Tumor volumes were measured by VOI on maximal-intensity-projection reconstructed images.

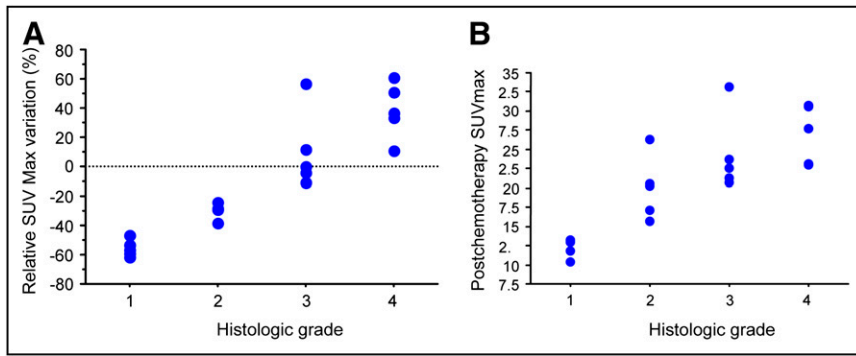


**FIGURE 4.** Correlation of tumor histologic response (Huvos) with SUVmax measured by  $^{18}\text{F}$ -FDG PET. (A) Scatter plot of relative SUVmax changes and tumor histologic response shows strong correlation of SUVmax change with histologic response ( $R^2 = 0.86$ ): a 40% decrease in SUVmax could distinguish good from partial responder (grade 1 from grade 2). (B) Scatter plot of SUVmax measured by  $^{18}\text{F}$ -FDG PET scan after chemotherapy correlates with histologic grade ( $R^2 = 0.94$ ). Postchemotherapy SUVmax less than 15 indicated good response to chemotherapy.

For this analysis, histologic response, relative SUVmax change, and postchemotherapy SUVmax from all animals studied were considered.

and bone tumors other than osteosarcoma (9,13,26). In fact, the predictive value of  $^{18}\text{F}$ -FDG PET in monitoring response to neoadjuvant chemotherapy has not been reported yet in osteosarcoma.

In our osteosarcoma model, we tested whether  $^{18}\text{F}$ -FDG PET correlated with the histologic response after neoadjuvant chemotherapy. Our results showed that ifosfamide-induced tumor response is associated with a decrease in tumor volume and an increase in tumor necrosis. When applying the prospective definitions of metabolic response according to the EORTC (19), we found that the changes of tumor volume and SUVmax were not correlated with tumor histologic response. This limitation could be explained in part because  $^{18}\text{F}$ -FDG PET does not allow distinguishing a necrotic area from osteoid matrix typically found in tumors after chemotherapy and whose localization can be confirmed only by histologic analysis. Another lack of sensitivity of  $^{18}\text{F}$ -FDG PET is illustrated by the fixation of radiotracer seen in fibrous scarring and tumor-infiltrated immune cells. Fibrous scarring and accumulation of infiltrating inflammatory cells within the tumor are modifications induced by chemotherapy that are commonly found in tumor response to chemotherapy. Glut-1 immunostaining by active immune cells led to the overestimation of tumor SUV changes and tumor volumes, a known issue responsible for the limited sensitivity of the technique in detecting tumor response to treatment (27). Nonetheless, we demonstrated that SUVmax measured at the completion of chemotherapy correlated strongly with histologic response and was thus able to distinguish good responders from partial responders. With the current race to design innovative PET radiopharmaceuticals, it is likely that other agents such as  $^{18}\text{F}$ -fluorothymidine, which measure more directly cell growth or death, or radiolabeled amino acids will be more effective than  $^{18}\text{F}$ -FDG in the evaluation of early tumor response (28).

## CONCLUSION

Taken together, our data validate  $^{18}\text{F}$ -FDG PET as an early marker of tumor response to neoadjuvant chemother-

apy in a relevant animal model of osteosarcoma that mimics its human counterpart. Our results suggest possible refinements to the EORTC classification (20) in which threshold rather than changes in SUVmax could be used to predict histologic response. Prospective studies are needed in patients with osteosarcoma to confirm the potential of metabolic imaging for the early detection of tumor response to neoadjuvant chemotherapy and its potential use as a decision-making tool to adapt treatment in poorly or even nonresponding patients. Ultimately, correlation between early metabolic imaging and long-term clinical outcome is warranted in patients with osteosarcoma.

## ACKNOWLEDGMENTS

We thank Dr. David Perol for support with statistical analysis, Jean Philippe Michot for technical advice, technicians from the Experimental Therapeutics Laboratory for their skilled assistance, the Institut Claude Bourgelat, and Stephane Martin at the Animage imaging platform for help and excellent care of the animals.

## REFERENCES

- Marec-Bérard C. Ostéosarcomes de l'enfant. *Oncologie*. 2006;8:546–550.
- Bielack SS, Kempf-Bielack B, Delling G, et al. Prognostic factors in high-grade osteosarcoma of the extremities or trunk: an analysis of 1,702 patients treated on neoadjuvant cooperative osteosarcoma study group protocols. *J Clin Oncol*. 2002;20:776–790.
- Clark JC, Dass CR, Choong PF. A review of clinical and molecular prognostic factors in osteosarcoma. *J Cancer Res Clin Oncol*. 2008;134:281–297.
- Huvos AG, Rosen G, Marcove RC. Primary osteogenic sarcoma: pathologic aspects in 20 patients after treatment with chemotherapy en bloc resection, and prosthetic bone replacement. *Arch Pathol Lab Med*. 1977;101:14–18.
- Hayashida Y, Yakushiji T, Awai K, et al. Monitoring therapeutic responses of primary bone tumors by diffusion-weighted image: initial results. *Eur Radiol*. 2006;16:2637–2643.
- Uhl M, Saueressig U, Koehler G, et al. Evaluation of tumour necrosis during chemotherapy with diffusion-weighted MR imaging: preliminary results in osteosarcomas. *Pediatr Radiol*. 2006;36:1306–1311.
- van der Woude HJ, Bloem JL, Holscher HC, et al. Monitoring the effect of chemotherapy in Ewing's sarcoma of bone with MR imaging. *Skeletal Radiol*. 1994;23:493–500.
- Mac Manus MP, Hicks RJ, Matthews JP, et al. Positron emission tomography is superior to computed tomography scanning for response-assessment after radical radiotherapy or chemoradiotherapy in patients with non-small-cell lung cancer. *J Clin Oncol*. 2003;21:1285–1292.

9. Evilevitch V, Weber WA, Tap WD, et al. Reduction of glucose metabolic activity is more accurate than change in size at predicting histopathologic response to neoadjuvant therapy in high-grade soft-tissue sarcomas. *Clin Cancer Res.* 2008;14:715–720.
10. Bastiaannet E, Groen H, Jager PL, et al. The value of FDG-PET in the detection, grading and response to therapy of soft tissue and bone sarcomas: a systematic review and meta-analysis. *Cancer Treat Rev.* 2004;30:83–101.
11. Juweid ME, Cheson BD. Positron-emission tomography and assessment of cancer therapy. *N Engl J Med.* 2006;354:496–507.
12. Schuetze SM, Rubin BP, Vernon C, et al. Use of positron emission tomography in localized extremity soft tissue sarcoma treated with neoadjuvant chemotherapy. *Cancer.* 2005;103:339–348.
13. Schuetze SM. Utility of positron emission tomography in sarcomas. *Curr Opin Oncol.* 2006;18:369–373.
14. Dutour A, Monteil J, Paraf F, et al. Endostatin cDNA/cationic liposome complexes as a promising therapy to prevent lung metastases in osteosarcoma: study in a human-like rat orthotopic tumor. *Mol Ther.* 2005;11:311–319.
15. Dutour A, Leclers D, Monteil J, et al. Non-invasive imaging correlates with histological and molecular characteristics of an osteosarcoma model: application for early detection and follow-up of MDR phenotype. *Anticancer Res.* 2007;27:4171–4178.
16. Allouche M, Delbrück HG, Klein B, et al. Malignant bone tumours induced by a local injection of colloidal radioactive <sup>144</sup>cerium in rats as a model for human osteosarcomas. *Int J Cancer.* 1980;26:777–782.
17. Hellwig D, Graeter TP, Ukena D, et al. <sup>18</sup>F-FDG PET for mediastinal staging of lung cancer: which SUV threshold makes sense? *J Nucl Med.* 2007;48:1761–1766.
18. Vera P, Ouvrier MJ, Hapdey S, et al. Does chemotherapy influence the quantification of SUV when contrast-enhanced CT is used in PET/CT in lymphoma? *Eur J Nucl Med Mol Imaging.* 2007;34:1943–1952.
19. Young H, Baum R, Cremerius U, et al. Measurement of clinical and subclinical tumour response using [<sup>18</sup>F]-fluorodeoxyglucose and positron emission tomography: review and 1999 EORTC recommendations. European Organization for Research and Treatment of Cancer (EORTC) PET Study Group. *Eur J Cancer.* 1999;35:1773–1782.
20. Coffin CM, Lowichik A, Zhou H. Treatment effects in pediatric soft tissue and bone tumors: practical considerations for the pathologist. *Am J Clin Pathol.* 2005;123:75–90.
21. Longhi A, Errani C, De Paolis M, Mercuri M, Bacci G. Primary bone osteosarcoma in the pediatric age: state of the art. *Cancer Treat Rev.* 2006;32:423–436.
22. de Geus-Oei LF, van der Heijden HF, Corstens FH, Oyen WJ. Predictive and prognostic value of FDG-PET in nonsmall-cell lung cancer: a systematic review. *Cancer.* 2007;110:1654–1664.
23. Nieweg OE, Pruijm J, van Ginkel RJ, et al. Fluorine-18-fluorodeoxyglucose PET imaging of soft-tissue sarcoma. *J Nucl Med.* 1996;37:257–261.
24. Brindle K. New approaches for imaging tumour responses to treatment. *Nat Rev Cancer.* 2008;8:94–107.
25. Minn H, Soini I. [<sup>18</sup>F]fluorodeoxyglucose scintigraphy in diagnosis and follow up of treatment in advanced breast cancer. *Eur J Nucl Med.* 1989;15:61–66.
26. Hawkins DS, Schuetze SM, Butrynski JE, et al. [<sup>18</sup>F]fluorodeoxyglucose positron emission tomography predicts outcome for Ewing sarcoma family of tumors. *J Clin Oncol.* 2005;23:8828–8834.
27. Fu Y, Maianu L, Melbert BR, Garvey WT. Facilitative glucose transporter gene expression in human lymphocytes, monocytes, and macrophages: a role for GLUT isoforms 1, 3, and 5 in the immune response and foam cell formation. *Blood Cells Mol Dis.* 2004;32:182–190.
28. Pio BS, Park CK, Pietras R, et al. Usefulness of 3'-[F-18]fluoro-3'-deoxythymidine with positron emission tomography in predicting breast cancer response to therapy. *Mol Imaging Biol.* 2006;8:36–42.